Nested high-resolution modeling of the impact of urbanization on regional climate in three vast urban agglomerations in China

Jun Wang,[1] Jinming Feng,[1] Zhongwei Yan,[1] Yonghong Hu,[2] and Gensuo Jia[1]

Received 4 June 2012; revised 17 September 2012; accepted 18 September 2012; published 1 November 2012.

[1] In this paper, the Weather Research and Forecasting Model, coupled to the Urban Canopy Model, is employed to simulate the impact of urbanization on the regional climate over three vast city agglomerations in China. Based on high-resolution land use and land cover data, two scenarios are designed to represent the nonurban and current urban land use distributions. By comparing the results of two nested, high-resolution numerical experiments, the spatial and temporal changes on surface air temperature, heat stress index, surface energy budget, and precipitation due to urbanization are analyzed and quantified. Urban expansion increases the surface air temperature in urban areas by about 1°C, and this climatic forcing of urbanization on temperature is more pronounced in summer and nighttime than other seasons and daytime. The heat stress intensity, which reflects the combined effects of temperature and humidity, is enhanced by about 0.5 units in urban areas. The regional incoming solar radiation increases after urban expansion, which may be caused by the reduction of cloud fraction. The increased temperature and roughness of the urban surface lead to enhanced convergence. Meanwhile, the planetary boundary layer is deepened, and water vapor is mixed more evenly in the lower atmosphere. The deficit of water vapor leads to less convective available potential energy and more convective inhibition energy. Finally, these combined effects may reduce the rainfall amount over urban areas, mainly in summer, and change the regional precipitation pattern to a certain extent.

Citation: Wang, J., J. Feng, Z. Yan, Y. Hu, and G. Jia (2012), Nested high-resolution modeling of the impact of urbanization on regional climate in three vast urban agglomerations in China, *J. Geophys. Res.*, *117*, D21103, doi:10.1029/2012JD018226.

1. Introduction

[2] The process of urbanization is one of the most extreme cases where humans have modified the earth system. Urbanization changes the land surface properties, such as albedo, emissivity, and thermal conductivity. Urban areas have a larger heat-storage capacity, Bowen ratio and an increased surface roughness in comparison with rural areas [*Oke*, 1982]. These differences lead to the modification of dynamic processes in the atmospheric boundary layer and the surface energy budget, which ultimately affects the regional climate in and around urban areas. In recent years, some researchers have used data and numerical models to study the impact of urbanization on synoptic process and regional climate change. For example, *Bornstein and Lin* [2000] used the surface meteorological network data around Atlanta and found that the urban heat island (UHI) could induce a convergence zone and tends to initiates storms. Also, *Shepherd et al.* [2002] suggested that the average increase in monthly rainfall could be as high as 28% within 30–60 km downwind of the metropolis. *Shem and Shepherd* [2009] found, using WRF that increased rainfall occurs downwind of Atlanta, which is consistent with many previous observational studies. *Shepherd et al.* [2010] conducted a case study and showed that simulations without a representation of the city produced less cumulative rainfall in the area to the west-northwest of Houston than simulations with the city represented. *Lin et al.* [2011] found that including the correct land use classification is crucial for UHI modeling studies and that the UHI effect plays an important role in accurately perturbing the thermal and dynamic processes. *Zhang et al.* [2009] conducted a series of numerical sensitivity experiments and found that the effects induced by the expanding urban surface are responsible for reducing precipitation over the Beijing area. All of these studies were based on observational data and selected representative cases to detect the urbanization effect on local and regional climate, while only a few considered the long-term climate effects caused by urbanization. *Trusilova et al.* [2008] simulated the UHI for January and July over a 6 year period and suggested that the conversion of land from rural

[1]Key Laboratory of Regional Climate-Environment Research for Temperate East Asia, Institute of Atmospheric Physics, Chinese Academy of Sciences, Beijing, China.
[2]Center for Earth Observation and Digital Earth, Chinese Academy of Sciences, Beijing, China.

Corresponding author: J. Feng, Key Laboratory of Regional Climate-Environment Research for Temperate East Asia, Institute of Atmospheric Physics, Chinese Academy of Sciences, Beijing 100029, China. (fengjm@tea.ac.cn)

0148-0227/12/2012JD018226

to urban results in statistically significant changes to precipitation and near-surface temperature over the perturbed areas of land. *Zhang et al.* [2010], following a similar approach to *Trusilova et al.* [2008], estimated the influence of urbanization on local and regional climate in Yangtze River Delta and suggested that the mean surface air temperature in urbanized areas increased on average by 0.45 ± 0.43°C in winter and 1.9 ± 0.55°C in summer. However, both studies were conducted with noncontinuous simulations and neither model had fine enough resolution to fully represent the surface characteristics of urban land. Given the complex interactions between urban land surfaces and the overlying atmosphere, long-term simulations including the seasonal cycle with finer spatial resolution and a more sophisticated urban canopy model are needed.

[3] Urbanization also brings about some bias to the accurate estimation of the global average temperature warming trend. Compared to the rural areas, urban areas experience extra warming due to the UHI effect [*Stone*, 2007]. Using the difference between trends in observed surface temperatures in the continental United States and the corresponding trends determined from NCEP-NCAR 50-year Reanalysis, *Kalnay and Cai* [2003] suggested that 0.27°C per century of the observed mean surface warming is due to urbanization and other land-use changes. But *Peterson* [2003] removed the biases caused by differences in elevation, latitude, time of observation, instrumentation, and nonstandard site location and showed that no statistically significant impact of urbanization could be found in the annual temperature data. *Ren et al.* [2007] found that annual urbanization-induced warming at the Beijing and Wuhan stations account for about $65 \sim 80\%$ and $40 \sim 61\%$ of the overall warming in the period of 1961–2000 and 1981–2000, respectively. However, based on an adjusted Beijing temperature series, *Yan et al.* [2010] suggested that the linear warming trend in Beijing during 1977–2006 was 0.78°C/decade. Comparing with several rural and less urban sites, *Yan et al.* [2010] suggested that the Beijing records include an urbanization-related warming bias, likely about 0.30°C/decade. Modeling studies may provide us some quantitative conclusions from a new perspective. However, existing global climate models (GCMs) employed for projections of future climate change do not account for urban areas, as the GCM's resolution is too coarse to describe the underlying surface characteristics of urban areas, which only cover a small fraction of Earth's surface. *Jin and Shepherd* [2005] indicated that adding an urban scheme into climate models, in order to scale the projections of global/regional climate to urban areas, becomes essential with the advance of satellite. *Lamptey* [2010] illustrated the gradual increases in turbulent fluxes over urban land areas and also pointed out the need to consider the urban landscape in regional studies. For these reasons, we need high-resolution regional modeling to study the climate change that occurs in urban areas.

[4] In the presence of global warming, the rapid process of urbanization has also resulted in many environment crises, such as prolonged heat waves and increased air pollution [*Robine et al.*, 2008; *Wang et al.*, 2007]. With more than half of the world's population residing in urban areas and with that percentage expected to increase [*Martine and Marshall*, 2007], investigating the impacts of urbanization can greatly help us to predict and respond to the problems caused by climate change in more scientifically useful ways. *Seto and Shepherd* [2009] indicated the considerable impact of urban land-use and land-cover changes on climate. *Stone* [2009] suggested that mitigating climate change could be better achieved by regulating land use change than by emissions reductions alone. Building on this idea, *Stone et al.* [2012] recommended that municipal and state governments broaden climate action plans to include urban-scale heat management strategies in addition to imposing greenhouse gas emission controls. China, particularly in the three vast urban agglomerations, represents the area of the world where the greatest increases in urban development have taken place since the 1950s. Some other regions may have experienced significant increases, but the areal extent of the changes is greatest across China. The impact of such a rapid urbanization process on regional climate is still unclear. Moreover, few studies have comparatively analyzed the urbanization effects in urban areas under different climatic regimes and employing differing energy consumption practices.

[5] With the aim of resolving these issues, in the present study we selected the coupled urban canopy model (UCM)/Weather Research and Forecasting model (WRF) and conducted relatively long-term simulations with nested high resolution to detect the impacts of urbanization on the regional climate in three vast urban agglomerations in China. Results derived from this effort can uncover how urbanization acts upon the regional climate and help to inform policy makers so that they can make wise decisions when dealing with weather and climate related issues occurring in and around highly developed areas. The remainder of this paper is organized as follows. The model and data are discussed in section 2, the results are presented in section 3, and the discussion and conclusion follows in section 4.

2. Model and Data

2.1. Numerical Model

[6] WRF is a next-generation, limited-area, nonhydrostatic, mesoscale modeling system with a terrain-following eta coordinate. The newest version of WRF has been coupled with the Noah land surface and UCM. The UCM is a single-layer model used to parameterize the effects of urban canopy geometry on the surface energy balance and low-level wind shear [*Kusaka et al.*, 2001; *Kusaka and Kimura*, 2004]. It estimates both the surface temperature and heat flux from three surface types: roof, wall and road and accurately reproduces the characteristics of the diurnal range and nocturnal cooling rates on surface air temperature [*Kusaka et al.*, 2001]. *Miao et al.* [2009] showed that the coupled WRF/Noah/UCM modeling system is able to reproduce the diurnal variation and spatial distribution of UHI in Beijing reasonably well. Such coupled models are able to capture the complex interaction between urban land surface characteristics and atmospheric processes.

[7] The model is configured for the current study with three levels of two-way nested grids having horizontal grid spacings of 30, 10 and 3.3 km. The locations of the nested urban domains are shown in Figure 1. The coarse outer domain, D01, comprises the whole of China and extends south into the South China Sea, while the intermediate resolution domain, D02, covers most of Eastern China. The

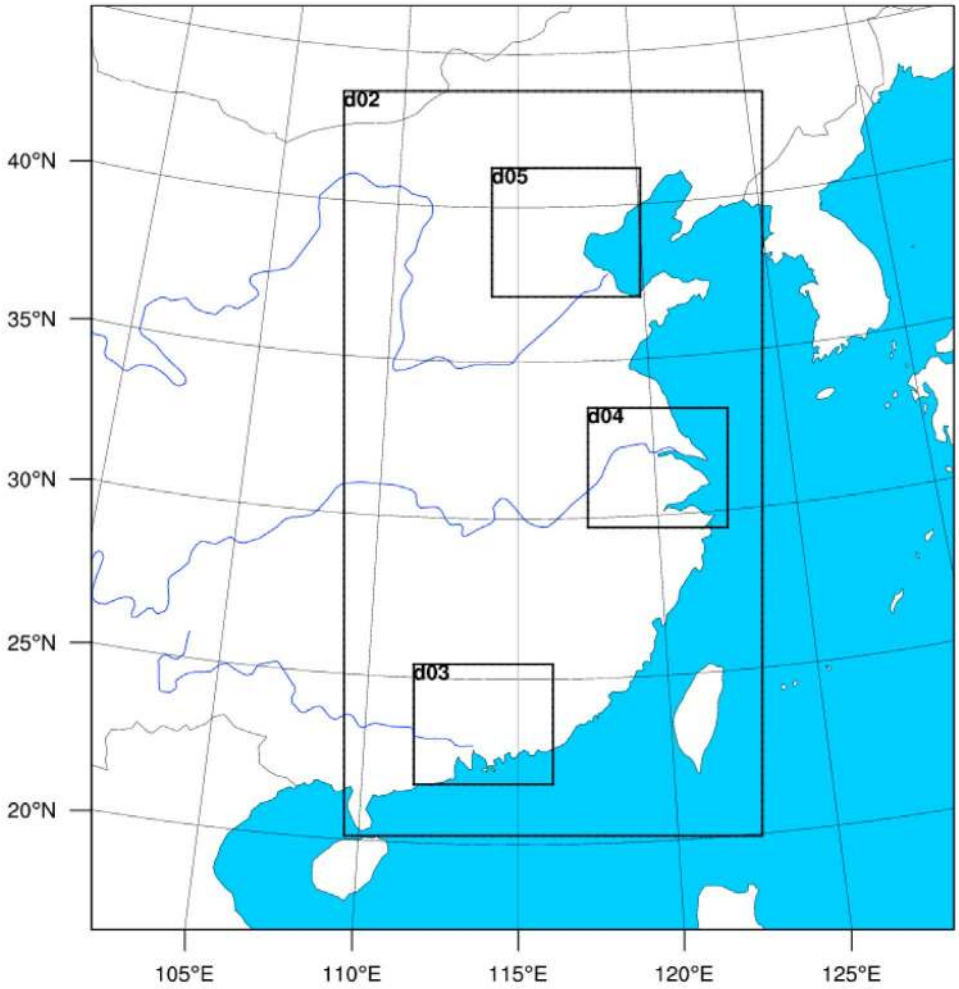

Figure 1. Configuration scheme for the nested model domains. Domains D3, D4, and D5 represent the three vast city agglomerations in China, namely the Pearl River Delta, the Yangtze River Delta, and the Beijing-Tianjin-Hebei metropolitan area, respectively.

inner high-resolution domains, D03, D04 and D05, are centered over the three vast urban agglomerations in the Pearl River Delta, the Yangtze River Delta and for the Beijing-Tianjin-Hebei metropolis, respectively. These areas have seen dramatic economic growth and substantial urban development has occurred since the reform process of China started in late 1978. A Lambert conformal conic projection is used for the model's horizontal coordinates. The model's vertical coordinate system employs 28 terrain-following eta levels from the surface to 50 hPa.

[8] The initial and boundary conditions (ICBCs) for the large-scale atmospheric field are given by the National Centers for Environmental Prediction's (NCEP) Global Final Analysis (FNL) 6 hourly data. The main physical parameterizations used include the new version of rapid radiative transfer model (RRTMG) [*Iacono et al.*, 2008], the WRF Single-Moment three-class scheme microphysical parameterization (WSM3) [*Hong et al.*, 2004], the new Kain-Fritsch convective parameterization (K-F) [*Kain*, 2004], the Yonsei University (YSU) planetary boundary layer (PBL) scheme [*Noh et al.*, 2003], and the Noah land surface model [*Chen and Dudhia*, 2001] with UCM [*Kusaka et al.*, 2001].

[9] By default, the urban land cover used by the WRF-UCM is classified into three subcategories (low-intensity residential, high-intensity residential and industrial/commercial). However, it should be noted that with the UCM activated, only the high-intensity residential land-use category was used to represent urban land cover in our simulations. Corresponding to this urban land-use type, WRF-UCM sets all urban grids to be covered by 90% urban cover (roof, wall and road), and 10% natural vegetation as default. As the density of buildings and roads in three vast urban agglomerations in China is very high, this default urban cover ratio is reasonable to some extent. Details of the parameters of urban canopy model are listed in Table 1. The SST and deep layer soil temperature are actively updated during the simulations. We set running time from 1 December 2006 to 1 January 2010 and the first month is considered as spin-up period and the outputs during this time are excluded from the following analysis.

Table 1. Urban Canopy Parameters From WRF for High-Intensity Residential Urban Land Use

Parameter[a]	Specific Values for High-Intensity Residential	Unit
h (building height)	7.5	m
l_{roof} (roof width)	9.4	m
l_{road} (road width)	9.4	m
C_R (heat capacity of roof)	1.0E6	J m^{-3} K^{-1}
C_W (heat capacity of wall)	1.0E6	J m^{-3} K^{-1}
C_G (heat capacity of road)	1.4E6	J m^{-3} K^{-1}
λ_R (thermal conductivity of roof)	0.67	J m^{-1} s^{-1} K^{-1}
λ_W (thermal conductivity of wall)	0.67	J m^{-1} s^{-1} K^{-1}
λ_G (thermal conductivity of road)	0.4004	J m^{-1} s^{-1} K^{-1}
α_R (surface albedo of roof)	0.20	fraction
α_W (surface albedo of wall)	0.20	fraction
α_G (surface albedo of road)	0.20	fraction
ε_R (surface emissivity of roof)	0.90	–
ε_W (surface emissivity of wall)	0.90	–
ε_G (surface emissivity of road)	0.95	–
Z_{0W} (roughness length for momentum over wall)	0.0001	m
Z_{0G} (roughness length for momentum over road)	0.01	m

[a] Z_{0R} is calculated from the urban morphological parameters by the UCM.

2.2. Land-Use Data

[10] The remote sensing product we used in this study was called the Model Land Cover Data sets version 1.0, obtained from Earth Observation of Climate Change (EOCC) research group (see http://green.tea.ac.cn/) [*Hu and Jia*, 2010]. The goal for this data set was to provide long-term land cover data for use in climate modeling to improve both the accuracy of model simulations and the effectiveness of their surface parameterizations. Multisource land cover products derived from satellite platforms, including USGS, MODIS land cover and China land use (CLU) data sets were used for a detailed investigation of the accuracy of the land cover classification for land cover data fusion. Three periods (1990, 2000 and 2009) were considered as the important nodes for land surface changes throughout China that have been caused by human activities over the last few decades. The IGBP land cover classification scheme was adopted in this data set, which was validated by high-resolution satellite imagery (Landsat TM/ETM+) to ensure its suitability and accuracy with the fraction cover value of each class being aggregated from 1 km resolution land cover products. Three spatial scales (3.3 km, 10 km and 30 km) were used to provide nesting input for climate model simulation over China and its main megametropolitan areas.

2.3. Case Design

[11] As our main objective was to explore the effects of urban expansion on regional climate, we designed two different urban land-use scenarios for numerical experiments. One experiment was a control run (S0) with all urban land cover fractions removed and other land cover fractions increased proportionately. If the urban land cover fraction in a grid cell was 100% we replaced the urban land cover fraction by interpolating from the fractions of surrounding land cover types. Another experiment was a sensitivity run (S1) where the urban land cover fractions were updated using the 2009 land use data described above to represent the current urbanization conditions with other land use fractions changed proportionately. In this scenario, the percentages of the area that was urbanized in the three urban domains were 13.09%, 17.92% and 11.92%, respectively. Figure 2 shows the detailed land use classification in the three high-resolution urban domains for the two modeling scenarios.

3. Results

3.1. Model Validation

[12] To validate the performance of the model, we compared the simulation results of S1 with observations from the CRU data set [*Mitchell and Jones*, 2005]. Figure 3 shows the comparison between simulated and observed monthly temperature and precipitation. Generally, the model simulates the seasonal variations of temperature and precipitation in the three domains quite well. However, compared to the observations, the simulated temperature has roughly a 2°C positive bias (Table 2) and the precipitation is overestimated in summer. A similar range of temperature error was also found in a study by *Kusaka and Hayami* [2006] using WRF simulations. Besides the intrinsic limitations of the simulation, the discrepancy between simulations and observations was caused by two primary factors. The first was that the resolution of the CRU data set (0.5°) is much coarser than the resolution used in simulation. Therefore, it was difficult for the observations to accurately depict the spatial distribution of surface air temperature and precipitation. Another was that we left out the effect of aerosols on radiative heat transfer, which may change the surface energy balance. Inclusion of the aerosol effects should act to reduce the surface air temperature [*Andreae et al.*, 2005] and help to eliminate the positive temperature bias.

[13] Table 2 gives the mean errors (ME) and correlation coefficients (CC) between the simulations and observations of temperature and precipitation in the three urban domains. The ME indicates the amount by which the model over or under predicts the mean magnitude of the observations. The CC shows the strength and direction of any linear relationship between simulation and observation. From Table 2, we can see that the model can generally generate realistic the regional-scale characteristics of temperature and precipitation. As we performed sensitivity experiments and compared the simulation of two cases with different urban land-use scenarios in this paper, we suggest cautiously that the bias between simulation and observation can be regarded as systematic model errors and these discrepancies may have little effect on the applicability of the conclusions.

3.2. Surface Air Temperature Change Due to Urbanization

[14] Figures 4a–4c show the differences in the surface air temperature between S1 and S0 in each of the three urban domains. Compared to S0, the regional average temperature of S1 increases over the three simulation domains are about 0.31°C, 0.44°C and 0.28°C, respectively. A stronger warming occurs in urbanized areas, which reach about 1.10°C, 1.31°C and 1.15°C. *Yan et al.* [2010] suggested that the Beijing temperature records include an urbanization-related warming bias of between 0.20 and 0.54°C/decade, likely about 0.30°C/decade, for 1977–2006. Assuming that the

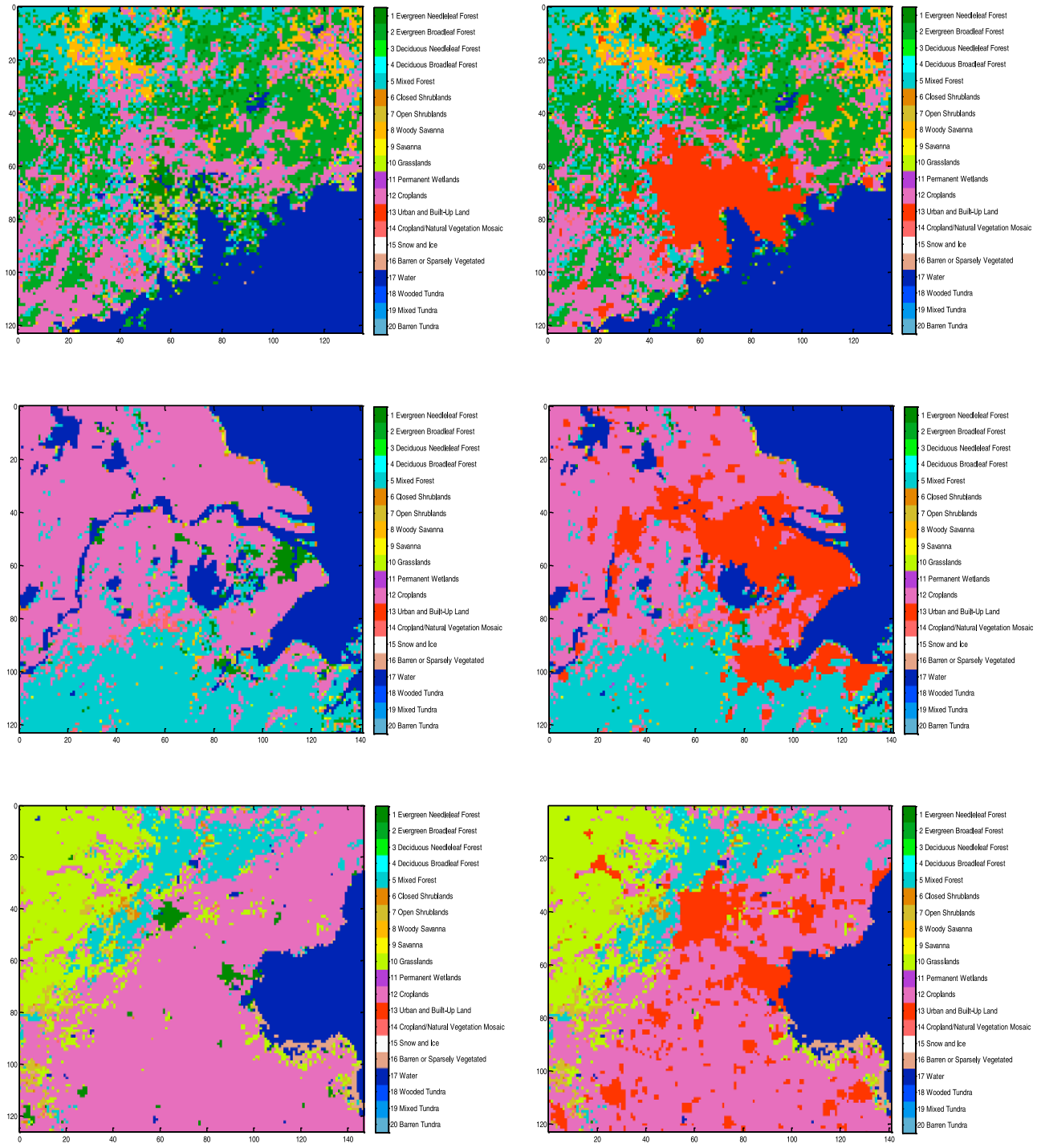

Figure 2. (left) Land-use classification contained in WRF-UCM for D3, D4, and D5, but with the urban type removed. (right) Land-use classification used in WRF-UCM for D3, D4, and D5, with the urban land-use fraction updated based on the Model Land Cover Data sets, version 1.0.

effect of Beijing's urbanization level on temperature before 1977 was very low, the urban-induced warming in Beijing could be as large as 0.9°C, which is close to the results of this paper. Based on the monthly mean surface air temperature during 1961–2000 from all of the weather and climate observation stations, *Ren et al.* [2008] found that the effect of urbanization on annual mean surface air temperature trends for large-city stations in northern China was 0.16°C/decade, which is slightly lower than the estimation of this paper. Considering that domain 5 represents the vast urban region around Beijing, whose urbanization level is higher than large city, the conclusion given by *Ren et al.* [2008] are also consistent with our simulated results.

[15] Figure 5a shows the seasonal variation of the surface air temperature difference due to urbanization. The urban temperature change in summer is almost twice that in winter

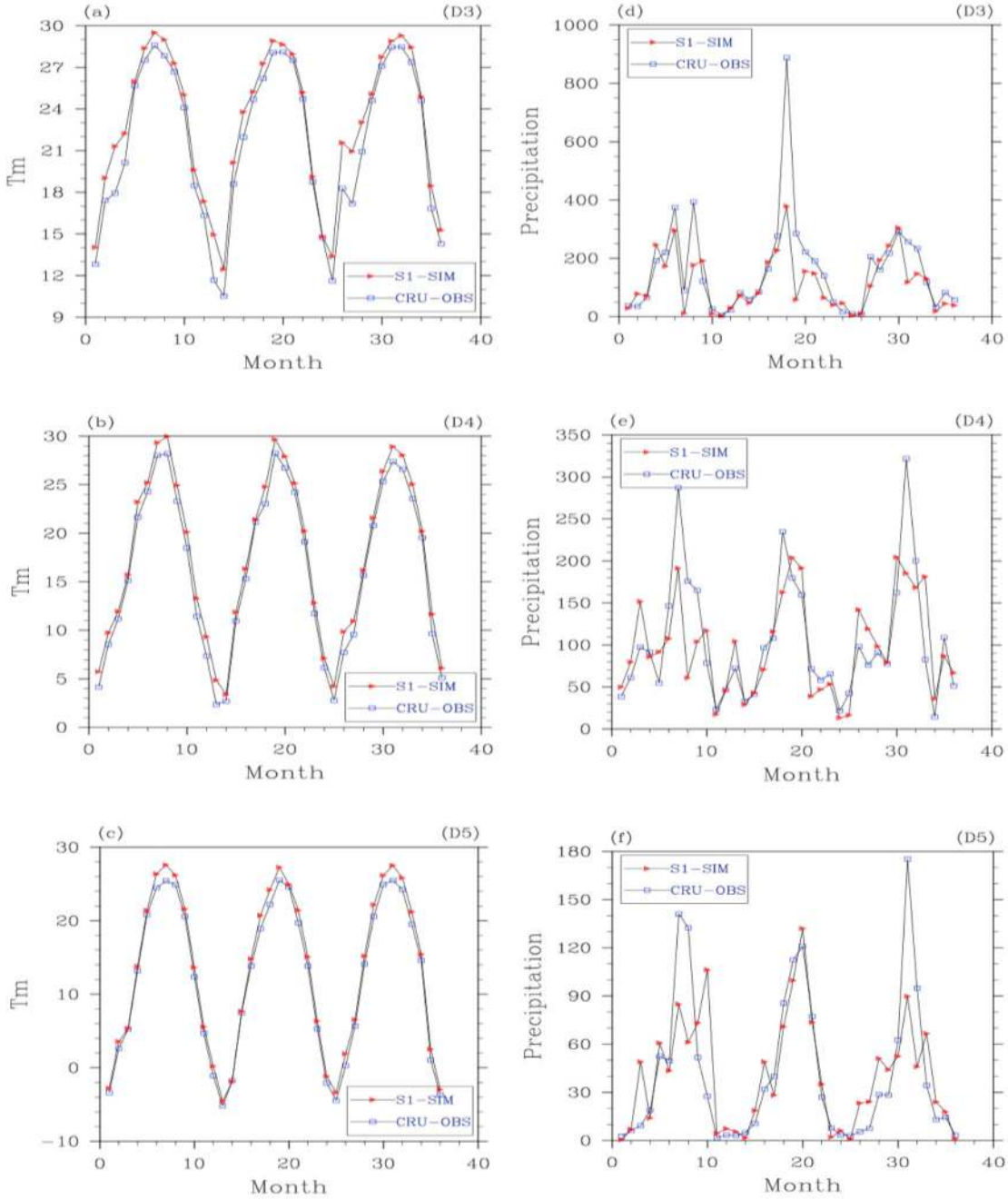

Figure 3. Annual variation of model-simulated (S1) and CRU observed 2 m (a–c) surface air temperature and (d–f) precipitation in D3 (Figures 3a and 3d), D4 (Figures 3b and 3e), and D5 (Figures 3c and 3f). The units for temperature are degrees Celsius, and the units for precipitation are millimeters.

(Table 3). The reason for this may be that the incident shortwave radiation is highest in summer, and this term dominates the energy budget of the surface.

[16] Previous studies have also documented that urbanization tends to increase the minimum temperature more than the maximum, thereby decreasing the diurnal temperature range. Figure 5b shows the surface air temperature change as a function of the time of day, and indicates that surface air temperatures increase more in LST 00 and LST 18 as a result of urbanization, which is consistent with the previous conclusions [*Kim and Baik*, 2005]. The larger increase of surface air temperature at night has several causes. In combination with the lower albedo of urban surfaces, which leads to a large energy absorption and storage during daytime, the limited availability of surface water reduces evaporative cooling of urban areas which limits the surface-to-atmosphere heat release, thereby extending it into the night hours.

3.3. Impact of Urbanization on Heat Stress Index

[17] Apart from excessive temperature anomalies, humidity may also play an important role on people's comfort and

Table 2. Mean Error, Spatial Correlation Coefficient, and Temporal Correlation Coefficient Between Surface Air Temperature and Precipitation Simulations and Observed Values[a]

	ME(T) (°C)	SCC(T)	ME(P)[b] (mm)	TCC(P)
D3	1.42	0.809[c]	−0.37 (−7.6%)	0.809[c]
D4	1.48	0.618[c]	0.14 (4.2%)	0.755[c]
D5	1.20	0.935[c]	0.01 (1.0%)	0.767[c]

[a]ME, mean error; P, precipitation; SCC, spatial correlation coefficient; T, surface air temperature; TCC, temporal correlation coefficient.
[b]The values in parentheses represent the percentages of mean error of simulated precipitation relative to observation.
[c]Statistically significant results at the 95% level ($\alpha = 0.05$).

health. The combination of high temperature and humidity reduces the efficiency of the human body's evaporative cooling and heat conduction mechanisms, which increases both morbidity and mortality. Previous studies used several common heat stress indices to address the combined effect of temperature and other factors on human health as a result of urbanization. In this study, we employ the Simplified Wet-Bulb Globe Temperature (W), defined by $W = 0.567\ T + 0.393e + 3.94$, where T is the temperature in °C, and e is the vapor pressure in hPa [*Willett and Sherwood*, 2012]. A W value less than 26 represents low health risk, W values between 26 and 28 means moderate risk, W values between 28 and 32 represents high risk and a W value more than 32 poses extreme health risk for people working or training under heat conditions [*Willett and Sherwood*, 2012]. The conversion of rural land cover to urban land cover leads to less available soil moisture and less vegetation cover, which may cause an "Urban Dry Island" effect over urbanized areas. The humidity deficit is a competing factor that may counteract the impact of temperature amplification on urban heat stress. So we need to estimate the relative role of temperature and humidity in determining the change of heat stress.

[18] Figures 4d–4f show the heat stress index changes due to urbanization in the three urban domains. These results indicate that the average heat stress index in urbanized areas increases by about 0.42, 0.53 and 0.54 units, respectively. The urban-induced humidity deficit partially offsets the enhanced heat stress due to the warming effect of urbanization. *Fischer et al.* [2012] used a global climate model including an urban canyon model to estimate the urban-rural heat stress contrast. They showed that, while the daytime heat stress index in urban areas is equal to that in rural areas, the heat stress in urban areas is about one unit higher than rural areas during the nighttime. Figure 6a shows the annually averaged diurnal variation of the change in the heat stress index due to urbanization, which clearly shows that the impact of urbanization on heat stress is more pronounced at night, in agreement with the results of *Fischer et al.* [2012]. Figure 6b shows the relationship between surface air temperature and heat stress index change due to urbanization. It indicates that the changes of heat stress intensity become slight larger as the surface air temperature increases and that the heat stress index changes caused by urbanization tend to be extremely high on days when daily mean air temperature exceeds about 25°C. This means that the amplification of heat stress due to urbanization is particularly pronounced during heat waves.

3.4. Changes on Surface Energy Budget

[19] Surface air temperature and moisture are influenced by several factors, such as incoming short-wave radiation, sensible heat flux, latent heat flux and advection. Therefore, studying the changes in surface energy balance due to urbanization is helpful to gain understanding of the regional climate change due to urban expansion.

[20] Figure 7 shows the changes in surface energy balance in the three urban domains. The underlying surface changes from other land use types to urban lead to an increase in sensible heat flux and a decrease in latent heat flux, which is consistent with many previous findings [e.g., *Guo et al.*, 2006; *Shem and Shepherd*, 2009]. The magnitude of the decrease in latent heat flux is larger than the increase in sensible heat flux so that the net ground flux changes slightly, which means that the net radiation over three domains decreases slightly due to urbanization. The net radiation is the sum of incoming short-wave, incoming long-wave radiation, reflected short-wave radiation and outgoing long-wave radiation over land surface. Figure 7 shows that the incoming short-wave radiation increases as a result of urbanization. To investigate the reasons, we analyzed the change of cloud fraction as a result of urbanization. Figure 8 shows the annually averaged diurnal variations of the change in cloud fraction due to urbanization. The cloud fraction decreases over all three urban domains after urbanization, with the decrease being especially pronounced in the morning. We suggest that the increase of solar radiation at the surface may be the result of this decrease in cloud fraction. However, changes in cloud fraction can't explain the increase of incoming long-wave radiation. The incoming long-wave radiation is mainly determined by the thermal radiation of atmosphere and cloud. We infer that the warmed air in the lower atmosphere may play a great role in the increase of incoming long-wave radiation. As for the decrease of reflected short-wave radiation, the main reasons for it may be the changes in surface properties, which decrease of albedo in urban areas, and the radiation capture effect of the urban canopy. Figure 7 also indicates that the outgoing long-wave radiation increases significantly after urbanization in the three urban domains. The change in outgoing long-wave radiation at the top of the atmosphere (OLR), due to increased emissivity and surface skin temperature, corroborates this change (not shown). We have further analyzed the seasonal changes of heat flux at the ground and found that this flux decreases in every season after the conversion of rural land cover to urban land cover, which is likely caused by the lower thermal conductivity of urban land surfaces.

3.5. Urbanization Influence on Precipitation

[21] Precipitation is a key factor in the global water cycle and a proxy for changing climate. Estimation of the effect of urbanization on precipitation becomes increasingly important for both climate change research and for its impact on human lives. Previous studies suggested that the UHI has a significant influence on mesoscale circulation and convection. For instance, using ground-based weather radar data, *Mote et al.* [2007] found that as a result of urbanization, areas in eastern metropolitan Atlanta have 30% more rainfall than areas to the west of the city. Further, both the amount

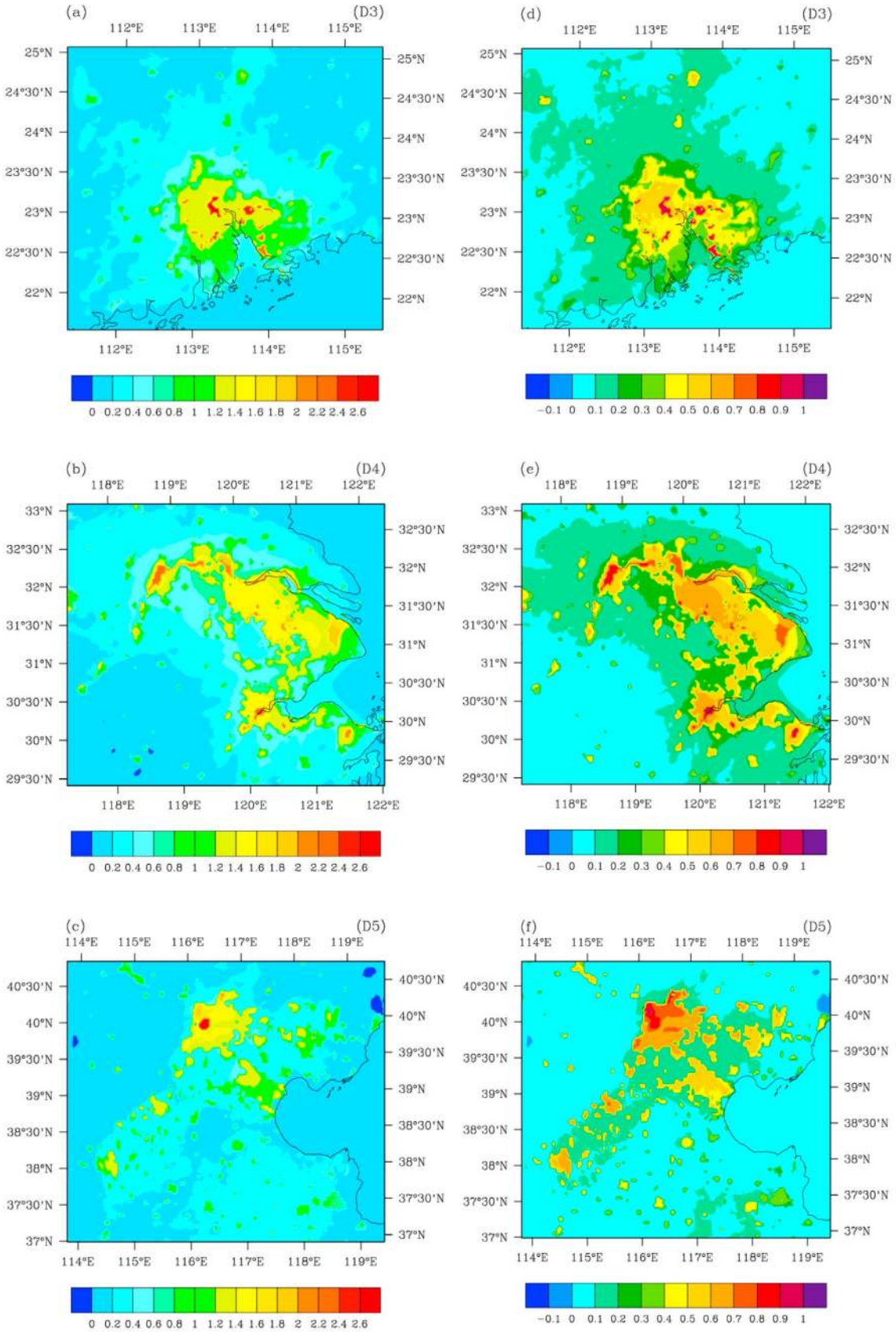

Figure 4. Spatial patterns of the change in (a–c) annual surface air temperature and (d–f) heat stress index due to urbanization in the three domains, D3 (Figures 4a and 4d), D4 (Figures 4b and 4e), and D5 (Figures 4c and 4f). The units for temperature are degrees Celsius, and the heat stress index is unitless.

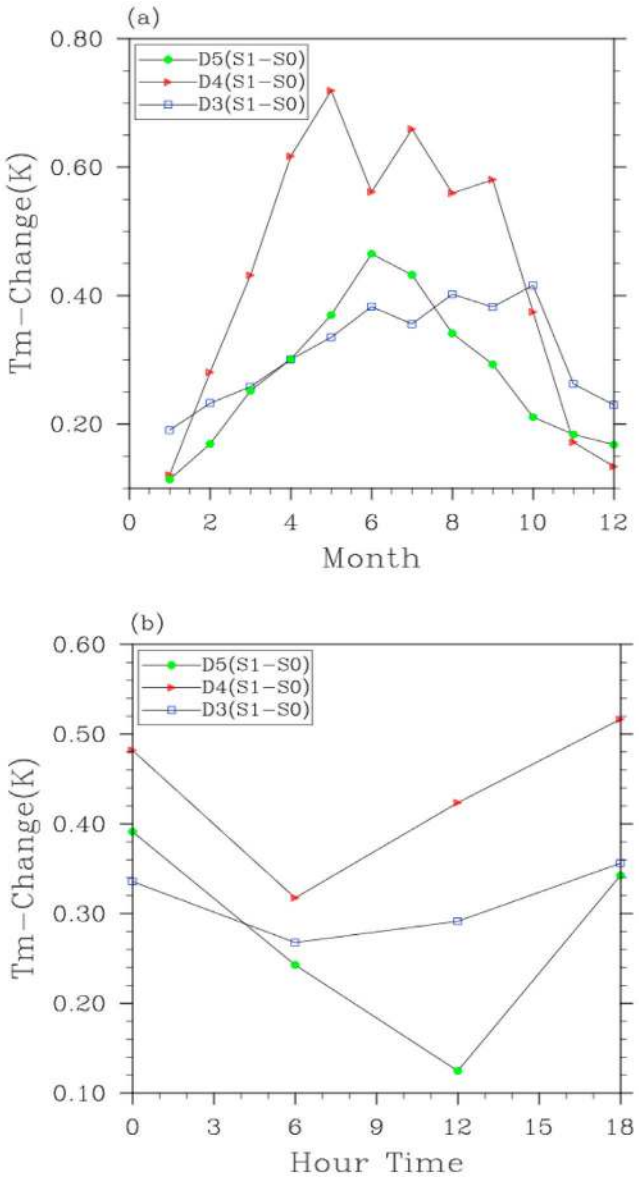

Figure 5. (a) Seasonal and (b) diurnal variations of the annual mean surface air temperature change due to urbanization (the blue, red, and green markers signify D3, D4, and D5, respectively).

and frequency of precipitation were enhanced as far as 80 km to the east of the urban core of Atlanta. *Chen et al.* [2007] suggested that urbanization in Taipei may contribute to an increase of more than 67% in the frequency of afternoon thunderstorms, and an increase of 77% in rainfall generated by thunderstorms. Through the analysis of radar imagery, *Niyogi et al.* [2011] found that storms split upwind of urban regions and merge again downwind. *Hand and Shepherd* [2009] analyzed the climatological sounding and reanalysis data and revealed that the downwind regions (the north-northeastern regions of Oklahoma City) are statistically wetter than other regions, confirming that precipitation modification due to urban effects may be more dominant than agricultural or topographic influences on weakly forced days. *Kishtawal et al.* [2010] suggested that the increase in the heavy rainfall climatology over the Indian monsoon region is a signature of an urban-induced rainfall anomaly. Traditional studies indicated that possible mechanisms for urbanization to impact precipitation and/or convection included: 1) enhanced convergence due to increased surface roughness in the urban area, 2) destabilization due to UHI perturbation of the planetary boundary layer. However, in this section, we provide a different view on the interaction between urban land use and the atmosphere that may cause the precipitation to be decreased over urban area.

[22] Figure 9 shows the changes due to urbanization of the annual and summer mean precipitation patterns in the three urban domains. The magnitude of precipitation decreases in the urbanized areas of D3 and D4, but increases slightly in the urbanized areas of D5. Overall, after urbanization the magnitude of precipitation decreases in urbanized area, but increases or remains unchanged in rural areas. The result that precipitation enhancement may occur downwind or in surrounding areas is consistent with previous studies. The patterns of change of annual precipitation are similar to those in summer. The reason why the patterns of change on annual precipitation are similar with summer is that the precipitation in East Asia is dominated by the Asian Monsoon, whose rainfall occurs mainly during the summertime. The results of previous studies [*Inoue and Kimura*, 2004; *Shem and Shepherd*, 2009; *Zhang et al.*, 2009; *Shepherd et al.*, 2010; *Niyogi et al.*, 2011] all showed that urbanization has a significant impact on the formation of clouds and thunderstorms and hence rainfall in summertime. Figure 10a shows the percentage change in regional monthly precipitation due to urbanization. At the regional level, urbanization has the greatest impact on summertime precipitation in the three urban domains. In particular, the percentage change in precipitation of D3 in August can reach nearly 20% (Table 4). In urbanized areas, the decreased precipitation in summer in D3 and D4 is readily apparent (Figure 10b). However, it is noteworthy that the precipitation governed by other larger-scale forcing that might act to mask the urban signature. To investigate the mechanism by which urban expansion impacts precipitation, we analyzed the change of the planetary boundary layer height (PBLH), convective available potential energy (CAPE) and convective inhibition energy (CIN) in summer. CAPE is defined as the accumulated buoyant energy from the level of free convection (LFC) to the equilibrium level (EL). CIN is defined as the accumulated negative buoyant energy from the parcel starting point to the LFC. Generally speaking, more CAPE and less CIN are more favorable for the initial and development of convection, which mainly occurs in summertime. Figure 11 shows the changes of PBLH due to urban land use in the three urban domains. The PBLH is elevated by more than 100 m over urban areas. We infer that the higher surface roughness and sensible heat flux may be the main causes of the increase in the PBLH. Figure 12 indicates that the average CAPE over the three urban domains decreases while the CIN increases due to urban land use. Further, we can see that urbanization tends to reduce the instability energy and decrease the rainfall amounts in summertime. However, summertime precipitation in D5 increases after urban expansion, which is different than in D3 and D4. Because there is more water vapor in D3 and D4 and less water vapor in D5 before urbanization, the decrease of water vapor due to

Table 3. Annual, Summer, and Winter Average Surface Air Temperature Change in the Three Urban Domains and Urban Areas

Time Period	Annual (°C)	JJA (°C)	DJF (°C)
D3	0.31	0.38	0.22
D4	0.44	0.59	0.18
D5	0.28	0.41	0.15
D3 (urban)	1.10	1.27	0.78
D4 (urban)	1.31	1.74	0.56
D5 (urban)	1.15	1.42	0.82

urbanization in D3 and D4 is much more than in D5. The negative effect of a small decrease of water vapor in D5 may be overwhelmed by other dynamical processes, which are discussed in following sections.

[23] UHI-sea breeze interactions are likely happening in the three urban regions and this may have an impact on the regional rainfall variability. In the days with an absence of large-scale synoptic forcing mechanisms, the sea breeze circulation may be well developed. We can use some diagnostic tools, such as the bulk Richardson shear number [*Carter et al.*, 2012] to detect the signal from urban–sea breeze interactions. Previous studies have demonstrated the role of UHI in the modification of sea breeze and revealed the complex interactions between them. For example, *Yoshikado* [1994] showed that the maximum vertical velocity or upward motion exiting the convergence zone of the sea breeze and the UHI circulation both grow over the inland part of Tokyo around midday. *Lo et al.* [2007] found that stronger UHI in the Pearl River Delta increases the differential temperature gradient between urbanized areas and the nearby ocean surface and hence enhances the mesoscale sea breeze circulation. *Carter et al.* [2012] suggested that, while coastal morphology can itself lead to complex sea breeze front structures, including preferred areas of vertical motion, the urban environment can have an impact on the evolution of the sea breeze mesoscale boundary. However, compared with stronger, more dominant synoptic flows, such as Asian Monsoon and the Westerlies, local circulations, like the sea breeze, are typically too shallow to be diagnosed. In long-term regional climate simulations, the sea breeze signal can be mitigated or washed out by the dominant synoptic flows. So the impact of the sea breeze or the UHI–sea breeze interaction on the changes to regional climate is very hard to detect. As previous case studies [e.g., *Shepherd et al.*, 2010; *Carter et al.*, 2012] indicated that the interaction between the UHI and the sea breeze can increase the strength of the vertical velocity anomaly and enhance the clouds and rainfall in urban areas, we suggest that these positive dynamic effects may be partly counteracted by the deficit of water vapor over urbanized areas.

[24] To explore the specific factors acting in the urban modification of precipitation, we analyzed the changes of the mesoscale circulation of the lower troposphere and the water vapor mixing ratio in summer due to urbanization. As shown by Figure 13, areas of enhanced convergence are associated with the urban environment. This is mainly due to the UHI thermal perturbation of the boundary layer and increased surface roughness of the urban environment. The enhanced convergence can lead to convective precipitation and/or cloud formation. However, apparently a deficit of water vapor also exists in urbanized areas which may counteract the effect of enhanced convergence on precipitation. Together these factors dominate the change of precipitation over urban area.

[25] The differences in the rainfall change due to urbanization between D3/D4 and D5 are noteworthy. The urban domains D3 and D4 are influenced by the strong East Asian monsoon, which brings in significant water vapor and high temperature in summer. The D5 domain lies in the northern part of China, which is also influenced by the monsoon, but is rather drier than the D3 and D4 domains. After urbanization, the deficits of water vapor in the lower troposphere in D3 and D4 are more than that in D5 (Figure 13). In addition,

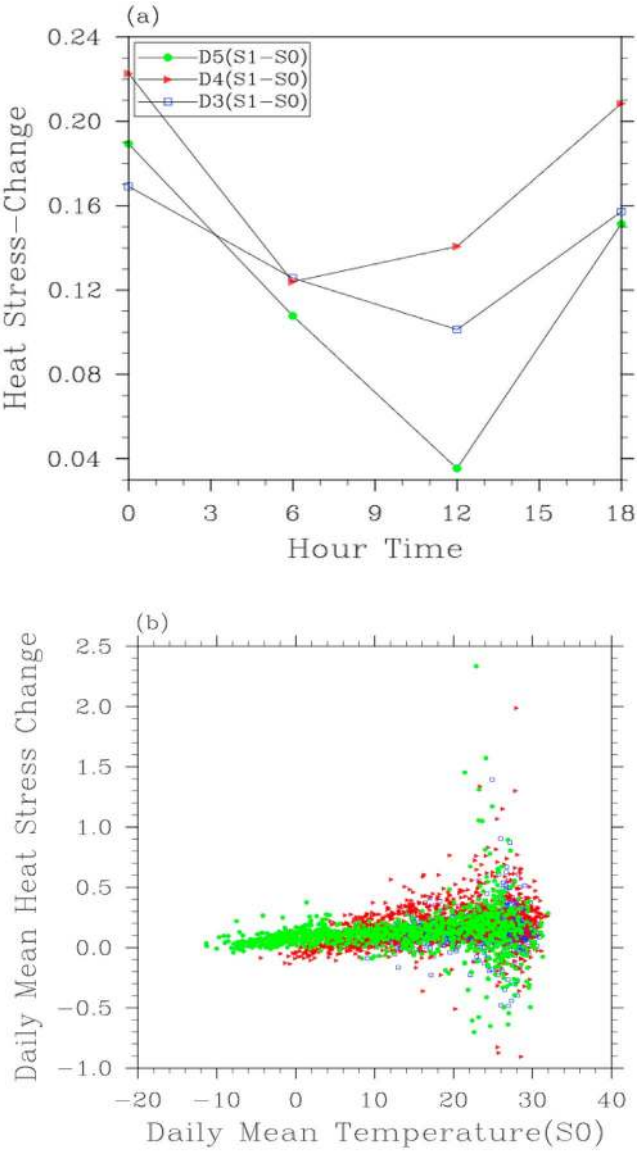

Figure 6. (a) Diurnal variations of the heat stress index change due to urbanization. (b) Relationship between temperature and heat stress index (the blue, red, and green markers signify D3, D4, and D5, respectively). The units for temperature are degrees Celsius, and the heat stress index is unitless.

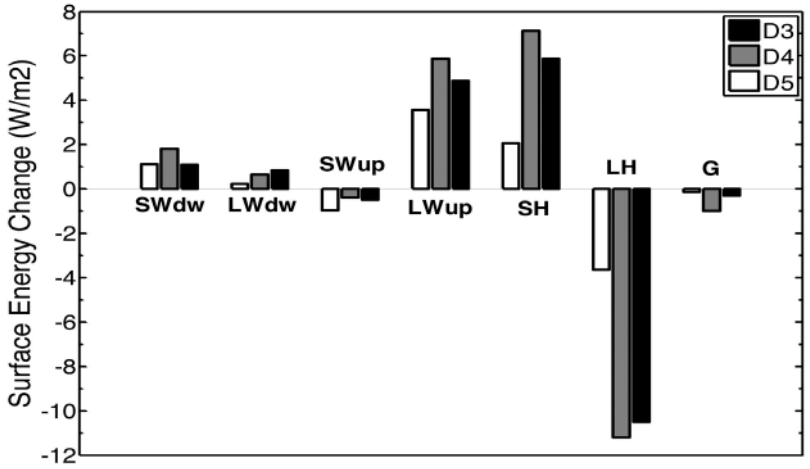

Figure 7. Changes in the surface energy balance (S1 minus S0) in the three urban domains. SWdw, downward short-wave flux; LWdw, long-wave flux; SWup, upward short-wave flux; LWup, long-wave flux at ground surface; SH, upward sensible heat flux; LH, latent heat flux; G, ground heat flux.

the size of urban agglomeration in D5 is smaller than those in D3 and D4. So the impact of urbanization on precipitation in D5 should be less significant than in D3 and D4. However, many scattered cities lie in the southern part of D5, which may have an influence on the mesoscale circulation. For although we see that the water vapor decreases little in the southeastern urban areas in D5 (Figure 13), due to the effect of the scattered cities, a cyclonic anomaly occurs there which may partly explain the increased precipitation in this area.

[26] Overall, through enhancing the surface sensible heat flux, the urbanization impact can deepen the PBL depth and strengthen the mixing of water vapor in the lower atmosphere over urban area. These changes, along with low evaporation from urban areas, inhibit the accumulation of water vapor in the PBL, decrease the CAPE and hence reduce the chances for deep convection to develop. These combined effects lead to the decrease of summertime rainfall over urban area. However, the increased convergence and/or cyclonic anomaly due to urban roughness may enhance the precipitation in these areas even when the water vapor in lower troposphere changes little. It reveals the important role that the water vapor plays in the modification of precipitation due to the impact of urbanization.

4. Discussion and Conclusion

[27] The three vast urban agglomerations in China have experienced remarkably rapid urbanization in the past three decades. Compared to global climate change, the regional climate change that has happened in urban areas may have more direct influence on humans. In this study, the Weather Research and Forecasting model coupled with the UCM was employed to quantify the degree to which extensive urban land use has forced changes in the regional climate over the three vast city agglomerations in China. We designed two types of urban land-use scenarios to represent rural (or pre-urban) land use and the current urban land-use conditions in 2009. Different from previous studies, we ran the regional climate model with very high, nested spatial resolution over a relatively long time period, so that the simulation results given in this paper could be more reliable and capture the effects upon the seasonal cycle of temperature and precipitation.

[28] Our simulation results suggest that the regional average surface air temperatures of the three vast city agglomerations D3, D4 and D5 increase by 0.31°C, 0.44°C and 0.28°C, respectively due to urbanization. Further, in the urban areas within these three domains the temperature increases can reach about 1.10°C, 1.31°C and 1.15°C. The urbanization causes a temperature increase that is about twice as large in summer than in winter and stronger at night than during the day. High temperature combined with high humidity increases human discomfort and leads to higher mortality. Studying the combined effects of urbanization on temperature and humidity is more beneficial than analyzing the temperature or humidity changes alone. In this paper, the

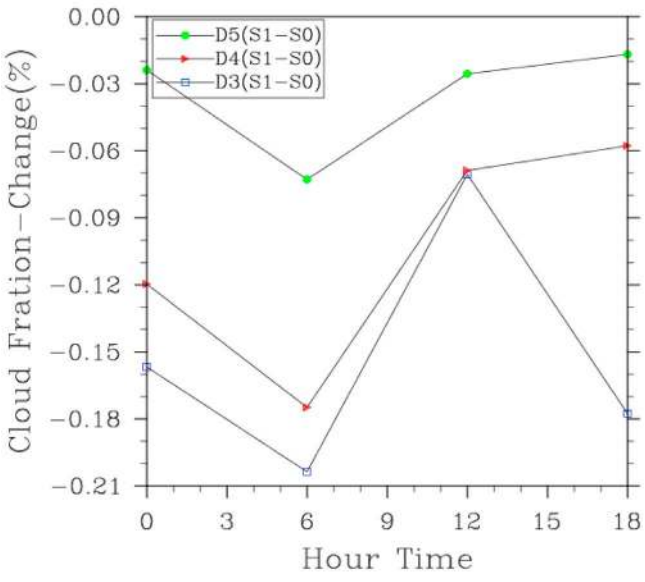

Figure 8. Diurnal variations of the annual mean cloud fraction change due to urbanization (the blue, red, and green markers signify D3, D4, and D5, respectively).

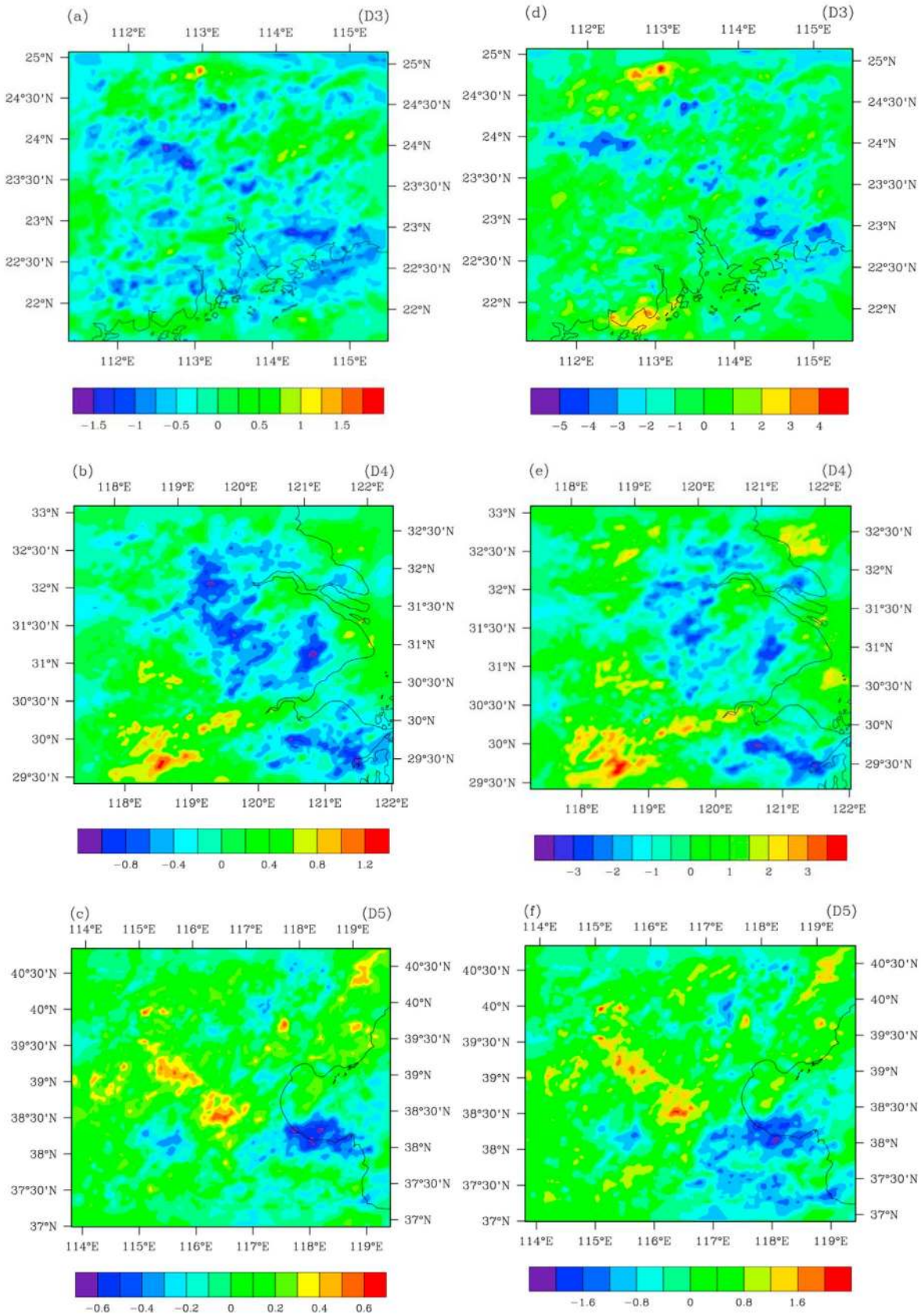

Figure 9. Changes in the (a–c) annual and (d–f) summer precipitation pattern (S1 minus S0) due to urbanization in D3 (Figures 9a and 9d), D4 (Figures 9b and 9e), and D5 (Figures 9c and 9f). The units are millimeters per day.

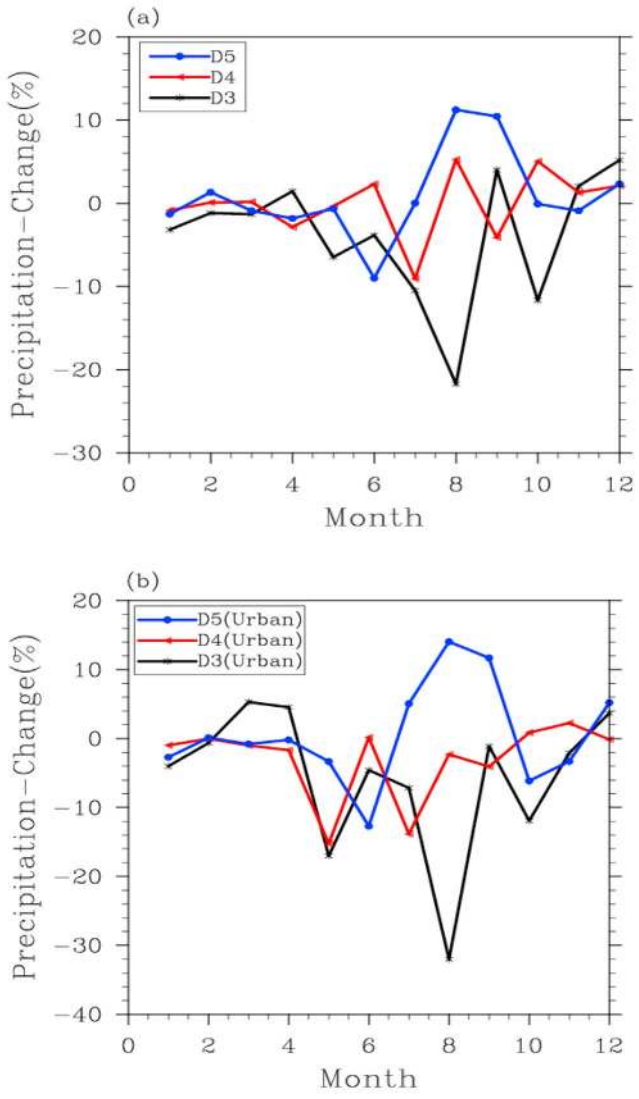

Figure 10. Percentage changes in monthly precipitation due to urbanization in (a) regional areas and (b) urban areas.

simulation results indicate that urban land use leads to an increase in the heat stress index by 0.42, 0.53 and 0.54 units in the three urbanized areas D3, D4 and D5, respectively. As with air temperature, heat stress is enhanced more during nighttime than during daytime. We also find that the change in heat stress due to urban expansion becomes more significant as the temperature increases and tends to be extremely large when temperature reaches a certain critical level.

[29] In terms of the surface energy balance, the simulation results show that urbanization produces less latent heat flux and more sensible heat flux, which leads to higher surface air temperatures and less water vapor in the lower troposphere. Urbanization also tends to decrease the regional cloud fraction, which may be the cause of the increased incoming short-wave radiation on the ground. Urbanization also decreases the albedo of land surfaces, which implies a decrease in the reflected solar radiation. Due to the increase of emissivity and surface skin temperature in urban areas, more long-wave radiation is emitted from the land surface to the atmosphere. Additionally, after urbanization the annual and seasonal ground heat fluxes are reduced, which may be caused by the lower thermal conductivity of urban land surfaces.

[30] Urban land use can change both the amount and pattern of regional precipitation. The rainfall in summer is disturbed sharply by increased urban land use. For example, in August the precipitation in D3 decreases by over 21% while in D5 it increases by over 11%. Analyzing the related physical variables, we find that the planetary boundary layer height is significantly elevated by urban expansion. This effect, which leads to more sensible heat flux and less latent flux, may cause the water vapor to be mixed more evenly which reduces the instability of the lower atmosphere. Studying the changes of convective available potential energy and convective inhibition energy, we suggest that the convective activities are strongly inhibited by urban land use, which ultimately causes the amount of summer precipitation to be reduced over urban area. What should be noted is that the summer precipitation amount in D5 is enhanced. We infer that another thermodynamic mechanism, other than those mentioned above, may be driving this change. Future work needs to fully investigate the relative role of the UHI-related dynamic processes and the deficits of water vapor in the modification of regional precipitation.

[31] Studying the urbanization impact on regional climate is helpful both in improving urban comfort level and in designing better disaster response plans for hazards such as heat waves and severe water shortages. Indeed, there are many factors not limited to urban land use that may have contributed to the urbanization impacts, such as anthropogenic waste heat and aerosol releases. Anthropogenic waste heat, for example, could contribute to the surface energy balance and the thermal structure of atmospheric boundary layer [*Flanner*, 2009]. *Block et al.* [2004] found a permanent warming due to anthropogenic heat emissions over affected areas ranging from 0.15 K over land area (with an additional 2 W m^{-2} anthropogenic heat flux) up to 0.5 K over the Ruhrarea (with additional 20 W m^{-2} anthropogenic heat flux). However, they suggested that anthropogenic heat flux

Table 4. Change in Precipitation in the Three Urban Domains and Urban Areas During the Summer and Fall

Month	May (%)	June (%)	July (%)	August (%)	September (%)	October (%)
D3	−6.48	−3.82	−10.48	−21.71	4.03	−11.66
D4	−0.36	2.33	−9.06	5.26	−4.09	5.06
D5	−0.63	−8.99	0.03	11.24	10.45	−0.07
D3(urban)	−17.03	−4.58	−7.16	−32.01	−1.11	−11.92
D4(urban)	−15.23	0.16	−13.82	−2.30	−4.08	0.86
D5(urban)	−3.34	−12.70	5.07	14.05	11.69	−6.14

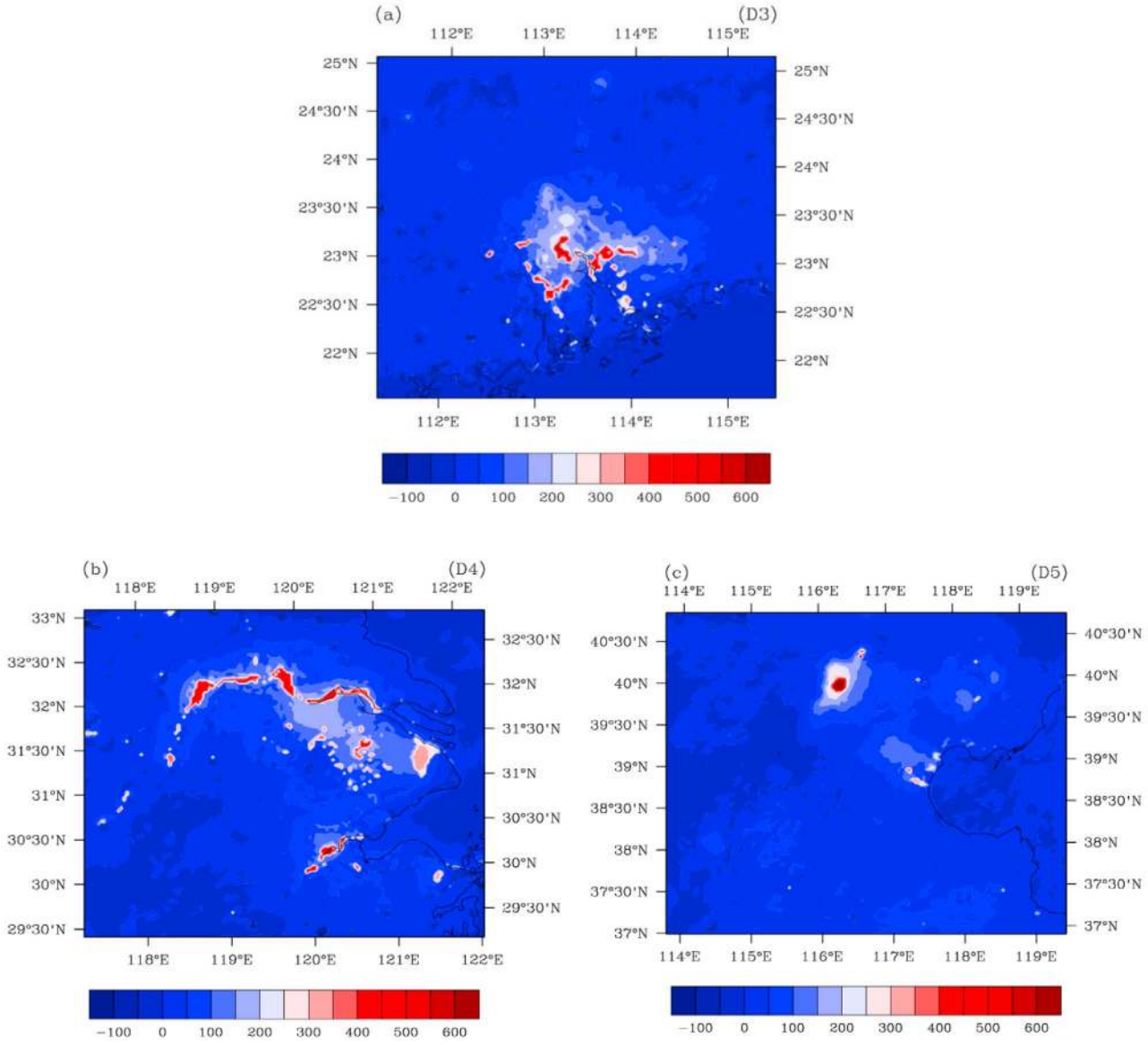

Figure 11. Change in the planetary boundary layer height in summer due to urbanization for (a) D3, (b) D4, and (c) D5. The units are meters.

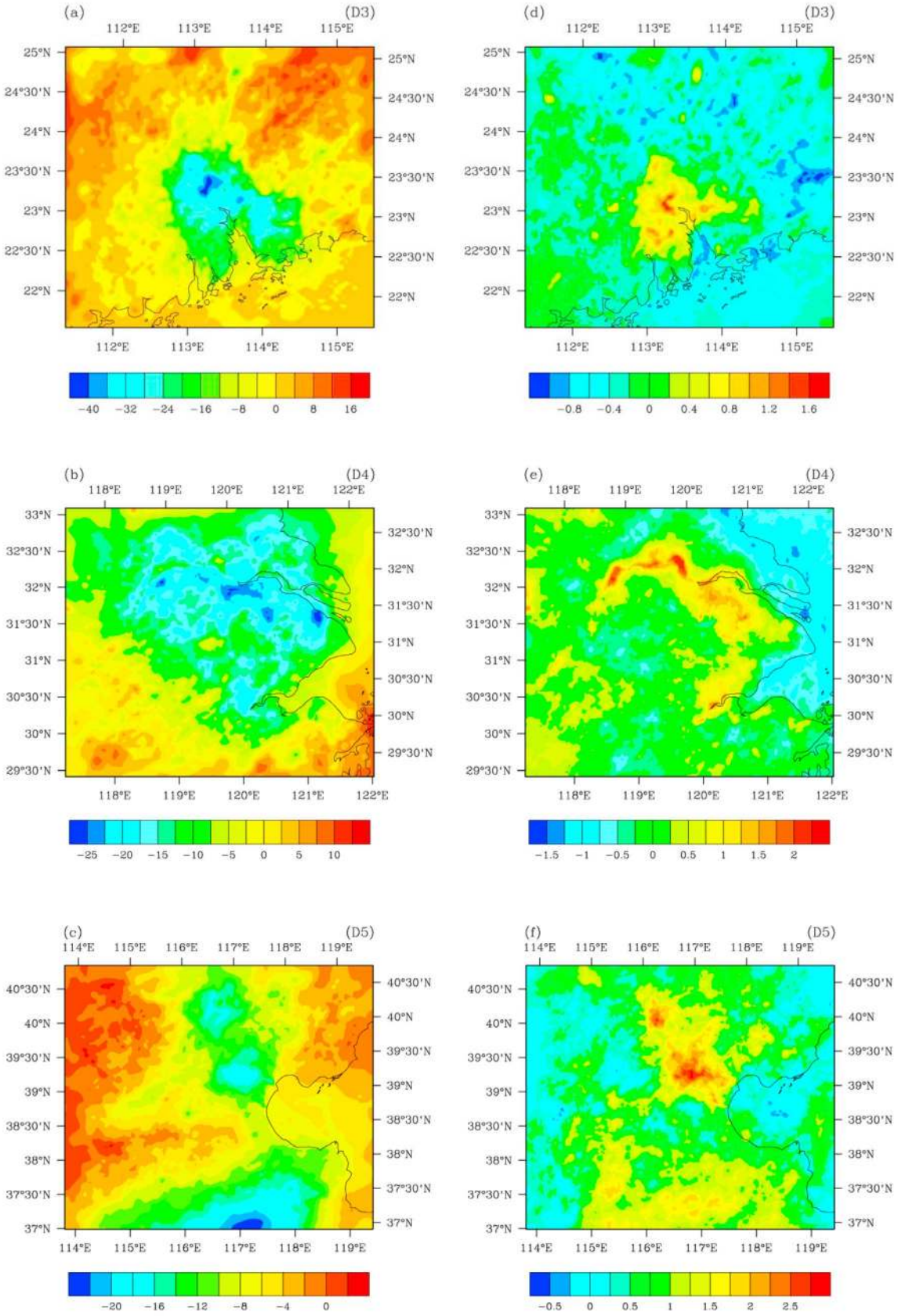

Figure 12. Changes in the (a–c) convective available potential energy and (d–f) convective inhibition energy in summer due to urbanization in D3 (Figures 12a and 12d), D4 (Figures 12b and 12e), and D5 (Figures 12c and 12f). The units are Joules per kilogram.

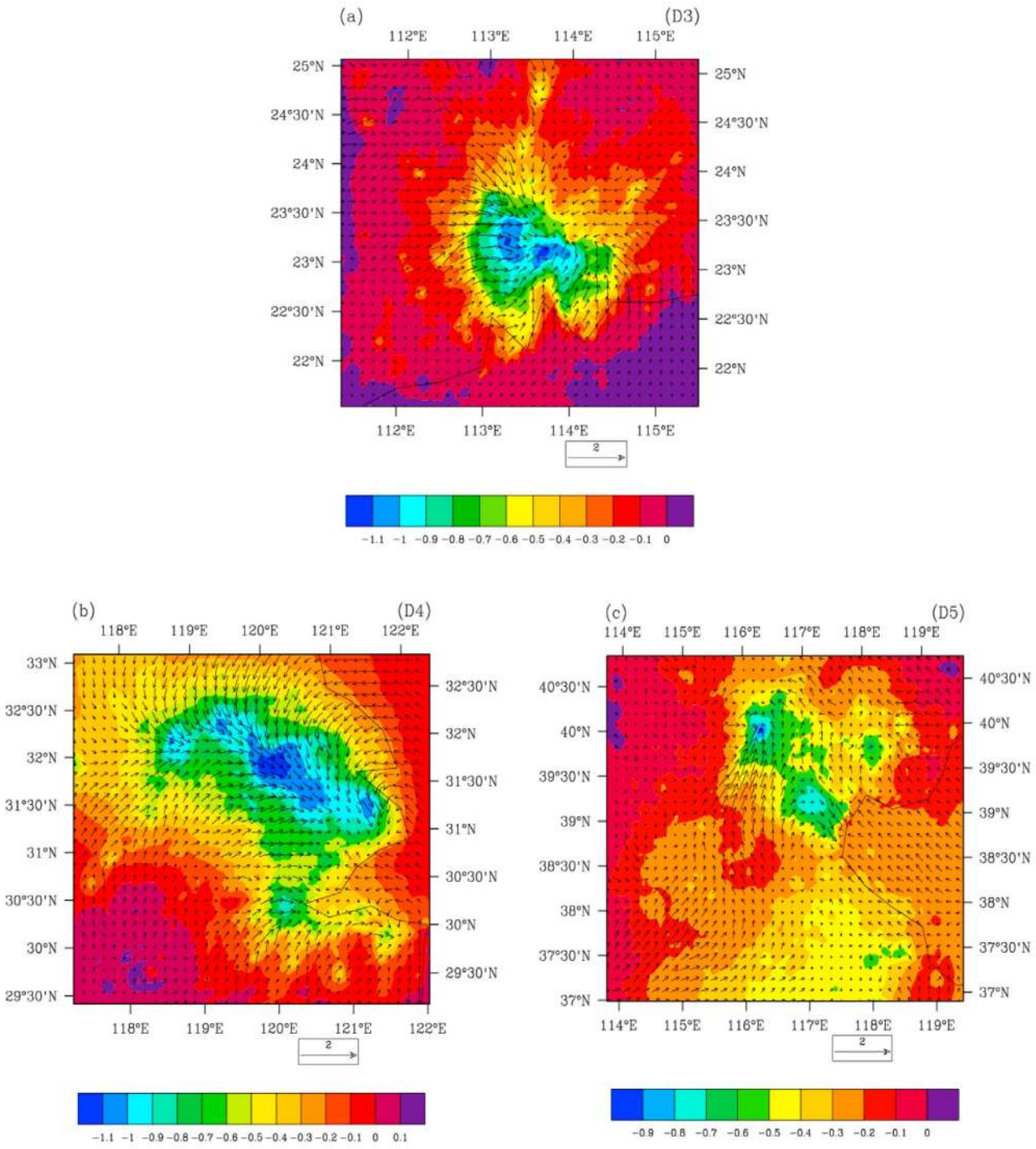

Figure 13. Changes in the circulation of the lower troposphere (at vertical level $\sigma = 0.988$ of the numerical model) and the water vapor mixing ratio in summer due to urbanization, for (a) D3, (b) D4, and (c) D5. The units for wind are meters per second, and the units for the water vapor mixing ratio are grams per kilogram.

did not affect rainfall as no significant variations in precipitation were found. However, their study only considered the effect of anthropogenic heat release on regional climate during winter, and the climatic effects in other seasons need to be quantified. This is especially important given that our results suggest the strongest rainfall changes occur in summer. Besides, anthropogenic heat flux induced planetary boundary layer expansion leads to a slight, but significant, increase in the atmospheric residence time of aerosols emitted from urban regions [*Flanner*, 2009]. In addition, pollutant releases (such as aerosols) can change the radiation process by its direct effect on absorption and modify the precipitation pattern by its indirect impacts [*Rosenfeld*, 2000]. *Rosenfeld et al.* [2007] established a relationship

between air pollutant release and the decrease in precipitation over a region in western China, and suggested that aerosol pollutants reduced rainfall in that region. *Jin et al.* [2005] found no clear relationship between monthly mean aerosol levels and rainfall measurements and suggested that in the summer the impact of aerosols may not play a significant role in changing the amount of urban rainfall. Given the large uncertainty in the impact of aerosols on climate and the complex interactions between the urban surface and the atmosphere, more work should be conducted to estimate the effect of pollutant emission on urban regional climate change. The research on urban land-use climatic forcing is a fundamental work that requires the consideration of many factors. To fully understand the impact of urbanization on regional climate change, future work will need to consider each of these factors and the interactions between them.

[32] **Acknowledgments.** This study was supported by the Strategic Priority Research Program-Climate Change: Carbon Budget and Relevant Issues of the Chinese Academy of Sciences (grant XDA05090000), NNSFC funds (grants 40975048 and 41075063), the National Key Program for Developing Basic Sciences of China (grant 2009CB421401), and the Innovation Key Program of the Chinese Academy of Sciences (grant KZCX2-EW-202).

References

Andreae, M. O., C. D. Jones, and P. M. Cox (2005), Strong present-day aerosol cooling implies a hot future, *Nature*, *435*, 1187–1190, doi:10.1038/nature03671.

Block, A., K. Keuler, and E. Schaller (2004), Impacts of anthropogenic heat on regional climate patterns, *Geophys. Res. Lett.*, *31*, L12211, doi:10.1029/2004GL019852.

Bornstein, R., and Q. Lin (2000), Urban heat islands and summertime convective thunderstorms in Atlanta: Three cases studies, *Atmos. Environ.*, *34*, 507–516, doi:10.1016/S1352-2310(99)00374-X.

Carter, M., J. M. Shepherd, S. Burian, and I. Jeyachandran (2012), Integration of lidar data into a coupled mesoscale-land surface model: A theoretical assessment of sensitivity of urban-coastal mesoscale circulations to urban canopy parameters, *J. Atmos. Oceanic Technol.*, *29*, 328–346, doi:10.1175/2011JTECHA1524.1.

Chen, F., and J. Dudhia (2001), Coupling and advanced land surface-hydrology model with the Penn State-NCAR MM5 modeling system. Part I: Model implementation and sensitivity, *Mon. Weather Rev.*, *129*, 569–585, doi:10.1175/1520-0493(2001)129<0569:CAALSH>2.0.CO;2.

Chen, T. C., S. Y. Wang, and M. C. Yen (2007), Enhancement of afternoon thunderstorm activity by urbanization in a Valley: Taipei, *J. Appl. Meteorol. Climatol.*, *46*, 1324–1340, doi:10.1175/JAM2526.1.

Fischer, E. M., K. W. Olesen, and D. M. Lawrence (2012), Contrasting urban and rural heat stress responses to climate change, *Geophys. Res. Lett.*, *39*, L03705, doi:10.1029/2011GL050576.

Flanner, M. G. (2009), Integrating anthropogenic heat flux with global climate models, *Geophys. Res. Lett.*, *36*, L02801, doi:10.1029/2008GL036465.

Guo, X. L., D. H. Fu, and J. Wang (2006), Mesoscale convective precipitation system modified by urbanization in Beijing City, *Atmos. Res.*, *82*, 112–126, doi:10.1016/j.atmosres.2005.12.007.

Hand, L. M., and J. M. Shepherd (2009), An investigation of warm-season spatial rainfall variability in Oklahoma City: Possible linkages to urbanization and prevailing wind, *J. Appl. Meteorol. Climatol.*, *48*, 251–269, doi:10.1175/2008JAMC2036.1.

Hong, S.-Y., J. Dudhia, and S.-H. Chen (2004), A revised approach to ice microphysical processes for the bulk parameterization of clouds and precipitation, *Mon. Weather Rev.*, *132*, 103–120, doi:10.1175/1520-0493(2004)132<0103:ARATIM>2.0.CO;2.

Hu, Y. H., and G. S. Jia (2010), Influence of land use change on urban heat island derived from multi-sensor data, *Int. J. Climatol.*, *30*, 1382–1395.

Iacono, M. J., J. S. Delamere, E. J. Mlawer, M. W. Shephard, S. A. Clough, and W. D. Collins (2008), Radiative forcing by long-lived greenhouse gases: Calculations with the AER radiative transfer models, *J. Geophys. Res.*, *113*, D13103, doi:10.1029/2008JD009944.

Inoue, T., and F. Kimura (2004), Urban effects on low-level clouds around the Tokyo metropolitan area on clear summer days, *Geophys. Res. Lett.*, *31*, L05103, doi:10.1029/2003GL018908.

Jin, M. L., and J. M. Shepherd (2005), Inclusion of urban landscape in a climate model: How can satellite data help?, *Bull. Am. Meteorol. Soc.*, *86*, 681–689, doi:10.1175/BAMS-86-5-681.

Jin, M. L., J. M. Shepherd, and M. D. King (2005), Urban aerosols and their variations with clouds and rainfall: A case study for New York and Houston, *J. Geophys. Res.*, *110*, D10S20, doi:10.1029/2004JD005081.

Kain, J. S. (2004), The Kain-Fritsch convective parameterization: An update, *J. Appl. Meteorol.*, *43*, 170–181, doi:10.1175/1520-0450(2004)043<0170:TKCPAU>2.0.CO;2.

Kalnay, E., and M. Cai (2003), Impact of urbanization and land-use change on climate, *Nature*, *423*, 528–531, doi:10.1038/nature01675.

Kim, Y. H., and J. J. Baik (2005), Spatial and temporal structure of the urban heat island in Seoul, *J. Appl. Meteorol.*, *44*, 591–605, doi:10.1175/JAM2226.1.

Kishtawal, C. M., D. Niyogi, M. Tewari, R. A. Pielke Sr., and J. M. Shepherd (2010), Urbanization signature in the observed heavy rainfall climatology over India, *Int. J. Climatol.*, *30*, 1908–1916, doi:10.1002/joc.2044.

Kusaka, H., and H. Hayami (2006), Numerical simulation of local weather for a high photochemical oxidant event using the WRF model, *JSME Int. J., Ser. B*, *49*, 72–77, doi:10.1299/jsmeb.49.72.

Kusaka, H., and F. Kimura (2004), Coupling a single-layer urban canopy model with a simple atmospheric model: Impact on urban heat island simulation for an idealized case, *J. Meteorol. Soc. Jpn.*, *82*, 67–80, doi:10.2151/jmsj.82.67.

Kusaka, H., K. Kondo, Y. Kikegawa, and F. Kimura (2001), A simple single-layer urban canopy model for atmospheric models: Comparison with multi-layer and slab models, *Boundary Layer Meteorol.*, *101*, 329–358, doi:10.1023/A:1019207923078.

Lamptey, B. (2010), An analytical framework for estimating the urban effect on climate, *Int. J. Climatol.*, *30*, 72–88, doi:10.1002/joc.1873.

Lin, C. Y., W. C. Chen, P. L. Chang, and F. Y. Sheng (2011), Impact of the urban heat island effect on precipitation over a complex geographic environment in northern Taiwan, *J. Appl. Meteorol. Climatol.*, *50*, 339–353, doi:10.1175/2010JAMC2504.1.

Lo, J. C. F., A. K. H. Lau, F. Chen, J. C. H. Fung, and K. K. M. Leung (2007), Urban modification in a mesoscale model and the effects on the local circulation in the Pearl River Delta region, *J. Appl. Meteorol. Climatol.*, *46*, 457–476, doi:10.1175/JAM2477.1.

Martine, G., and A. Marshall (2007), State of world population 2007: Unleashing the potential of urban growth, report, U.N. Popul. Fund, New York.

Miao, S. G., F. Chen, M. A. Lemone, M. Tewari, Q. C. Li, and Y. C. Wang (2009), An observational and modeling study of characteristics of urban heat island and boundary layer structures in Beijing, *J. Appl. Meteorol. Climatol.*, *48*, 484–501, doi:10.1175/2008JAMC1909.1.

Mitchell, T. D., and P. D. Jones (2005), An improved method of constructing a database of monthly climate observations and associated high-resolution grids, *Int. J. Climatol.*, *25*, 693–712, doi:10.1002/joc.1181.

Mote, T. L., M. C. Lacke, and J. M. Shepherd (2007), Radar signatures of the urban effect on precipitation distribution: A case study for Atlanta, Georgia, *Geophys. Res. Lett.*, *34*, L20710, doi:10.1029/2007GL031903.

Niyogi, D., P. Pyle, M. Lei, S. P. Arya, C. M. Kishtawal, M. Shepherd, F. Chen, and B. Wolfe (2011), Urban modification of thunderstorms: An observational storm climatology and model case study for the Indianapolis urban region, *J. Appl. Meteorol. Climatol.*, *50*, 1129–1144, doi:10.1175/2010JAMC1836.1.

Noh, Y., W. G. Cheon, S.-Y. Hong, and S. Raasch (2003), Improvement of the K-profile model for the planetary boundary layer based on large eddy simulation data, *Boundary Layer Meteorol.*, *107*, 401–427, doi:10.1023/A:1022146015946.

Oke, T. R. (1982), The energetic basis of the urban heat island, *Q. J. R. Meteorol. Soc.*, *108*, 1–24.

Peterson, T. C. (2003), Assessment of urban versus rural in situ surface temperatures in the contiguous United States: No difference found, *J. Clim.*, *16*, 2941–2959, doi:10.1175/1520-0442(2003)016<2941:AOUVRI>2.0.CO;2.

Ren, G. Y., Z. Y. Chu, Z. H. Chen, and Y. Y. Ren (2007), Implications of temporal change in urban heat island intensity observed at Beijing and Wuhan stations, *Geophys. Res. Lett.*, *34*, L05711, doi:10.1029/2006GL027927.

Ren, G. Y., Y. Q. Zhou, Z. Y. Chu, J. X. Zhou, A. Y. Zhang, J. Guo, and X. F. Liu (2008), Urbanization effects on observed surface air temperature trends in North China, *J. Clim.*, *21*, 1333–1348, doi:10.1175/2007JCLI1348.1.

Robine, J., S. Cheung, S. Le Roy, H. Van Oyen, C. Griffiths, J. Michel, and F. Herrmann (2008), Death toll exceeded 70,000 in Europe during the summer of 2003, *C. R. Biol.*, *331*, 171–178, doi:10.1016/j.crvi.2007.12.001.

Rosenfeld, D. (2000), Suppression of rain and snow by urban and industrial air pollution, *Science*, *287*, 1793–1796, doi:10.1126/science.287.5459.1793.

Rosenfeld, D., J. Dai, X. Yu, X. Xu, X. Yang, C. L. Du, and Z. Yao (2007), Inverse relations between amounts of air pollution and orographic precipitation, *Science*, *315*, 1396–1398, doi:10.1126/science.1137949.

Seto, K. C., and J. M. Shepherd (2009), Global urban land-use trends and climate impacts, *Curr. Opin. Environ. Sustainability*, *1*, 89–95, doi:10.1016/j.cosust.2009.07.0 12.

Shem, W., and M. Shepherd (2009), On the impact of urbanization on summertime thunderstorms in Atlanta: Two numerical model case studies, *Atmos. Res.*, *92*, 172–189, doi:10.1016/j.atmosres.2008.09.013.

Shepherd, J. M., H. Pierce, and A. J. Negri (2002), Rainfall modification by major urban areas: Observations from spaceborne rain radar on the TRMM satellite, *J. Appl. Meteorol.*, *41*, 689–701, doi:10.1175/1520-0450(2002)041<0689:RMBMUA>2.0.CO;2.

Shepherd, J. M., W. M. Carter, M. Manyin, D. Messen, and S. Burian (2010), The impact of urbanization on current and future coastal precipitation: A case study for Houston, *Environ. Plann.*, *37B*, 284–304.

Stone, B. (2007), Urban and rural temperature trends in proximity to large U.S. cities: 1951–2000, *Int. J. Climatol.*, *27*, 1801–1807, doi:10.1002/joc.1555.

Stone, B. (2009), Land use as climate change mitigation, *Environ. Sci. Technol.*, *43*, 9052–9056, doi:10.1021/es902150g.

Stone, B., J. Vargo, and D. Habeeb (2012), Managing climate change in cities: Will climate action plans work?, *Landscape Urban Plann.*, *107*, 263–271, doi:10.1016/j.landurbplan.2012.05.014.

Trusilova, K., M. Jung, G. Churkina, U. Karstens, M. Heimann, and M. Claussen (2008), Urbanization impacts on the climate in Europe: Numerical experiments by the PSU-NCAR mesoscale model (MM5), *J. Appl. Meteorol. Climatol.*, *47*, 1442–1455, doi:10.1175/2007JAMC1624.1.

Wang, X. M., W. S. Lin, L. M. Yang, R. R. Deng, and H. Lin (2007), A numerical study of the influences of urban land-use change on ozone distribution over the Pearl River Delta region, China, *Tellus, Ser. B*, *59*, 633–641.

Willett, K. M., and S. C. Sherwood (2012), Exceedance of heat index thresholds for 15 regions under a warming climate using the wet-bulb globe temperature, *Int. J. Climatol.*, *32*, 161–177, doi:10.1002/joc.2257.

Yan, Z. W., Z. Li, Q. X. Li, and P. D. Jones (2010), Effects of site change and urbanisation in the Beijing temperature series 1977–2006, *Int. J. Climatol.*, *30*, 1226–1234, doi:10.1002/joc.1971.

Yoshikado, H. (1994), Interaction of the sea breeze and urban heat islands of different sizes and location, *J. Meteorol. Soc. Jpn.*, *72*, 139–142.

Zhang, C. L., F. Chen, S. G. Miao, Q. C. Li, X. A. Xia, and C. Y. Xuan (2009), Impacts of urban expansion and future green planting on summer precipitation in the Beijing Metropolitan area, *J. Geophys. Res.*, *114*, D02116, doi:10.1029/2008JD010328.

Zhang, N., Z. Q. Gao, X. M. Wang, and Y. Chen (2010), Modeling the impacts of urbanization on the local and regional climate in Yangtze River Delta, China, *Theor. Appl. Climatol.*, *68*, 67–73, doi:10.1007/s007040170054.